Pure Appl. Geophys. 180 (2023), 1121–1142

https://doi.org/10.1007/s00024-022-03225-3

Pure and Applied Geophysics

Performance of the CORDEX-SA Regional Climate Models in Simulating Summer Monsoon Rainfall and Future Projections over East India

Vasundhara Barde,[1,4] M. M. Nageswararao,[2,3] U. C. Mohanty,[1,5] and R. K. Panda[1,5]

Abstract—The Indian summer monsoon rainfall (ISMR, June–September) is an important factor in agricultural planning and the Indian economy. The ISMR over East India (EI: Chhattisgarh-Bihar-Jharkhand-Odisha) is particularly significant, and it can have an impact on the country's average ISMR. The current study examined projected changes in ISMR over EI with two emission scenarios, RCP4.5 and RCP8.5, for near (2017–2040) and far-future (2041–2070) projections using a set of ten CORDEX-SA Regional Climate Model (RCMs). To begin, the performance of raw and bias-corrected ISMR over EI outputs from ten CORDEX-SA RCMs was compared to a high-resolution (0.25° × 0.25°) gridded rainfall analysis dataset from the India Meteorological Department (IMD) over the hindcast period (1971–2005). Following that, bias-corrected results were used to calculate ISMR projections over EI for the near and distant futures. Most RCMs, according to the findings, can imitate the spatial pattern of ISMR across EI but are restricted in their ability to capture actual magnitudes. Notably, RCM prediction skill increased greatly after employing various bias-correction approaches, the quantile mapping (QQM) bias-correction technique outperformed other current conventional bias correction methods, and the QQM technique was employed for ISMR future projections using RCP4.5 and RCP8.5 emission scenarios. The analysis of ISMR projections over EI reveals that there will be more deficit rainfall years in the short term while more excess rainfall years in the far future.

Keywords: CORDEX-SA, Indian summer monsoon, East India, RCP, Future projections, Global warming.

[1] School of Earth, Ocean, and Climate Sciences, Indian Institute of Technology Bhubaneswar, Argul, Jatani, Odisha 752050, India. E-mail: ucmohanty@iitbbs.ac.in
[2] NOAA Center for Weather and Climate Prediction, NCEP EMC, University Research Court, College Park, MD 20740, USA.
[3] CPAESS, University Corporation for Atmospheric Research (UCAR), Boulder, CO, USA.
[4] Indian Institute of Geomagnetism, Mumbai 410218, India.
[5] Centre for Climate Smart Agriculture (CCSA), Shikha 'O' Anusandhan University, Bhubaneswar, India.

1. Introduction

Understanding and predicting Indian summer monsoon rainfall (June through September (JJAS); ISMR) are essential because this is the main rainy season in India and accounts for approximately 70–90% of annual rainfall in most places (Kumar et al., 2013). Several attempts have previously been made to predict the seasonal and year-to-year variability of ISMR (Acharya et al., 2013; Barde et al., 2020; Kumar et al., 2013; Mishra et al., 2012; Mohanty et al., 2019). In recent years, India's seasonal rainfall has significantly reduced, with a considerable reduction over the monsoon core zone and India's Gangetic Plains (Kulkarni, 2012; Das et al., 2016; Roxy, 2017; Barde et al., 2020). India is located in the South Asian Monsoon region, which has a long history of extreme weather and climate events. A regional-scale study is especially important in India because of its diverse geographical nature. Furthermore, megacities such as Mumbai, Chennai, and Bengaluru have experienced frequent extreme rainfall events, while the Indo-Gangetic Plains have recently experienced frequent drought conditions (Kumar et al., 2008; Sahany et al., 2010; Seenirajan et al., 2017; Barde et al., 2020). As a result, reliable seasonal rainfall projections at the regional level are critical for adopting new technologies in various climate risk sectors in the current changing climate.

Global climate models (GCMs) are widely used for climate change analysis and projections, but the projections are global in scope and have a coarse resolution, making regional-scale processes difficult to simulate (Sannan et al., 2020; Taylor et al., 2012). To obtain information at a finer scale, statistical and dynamical downscaling techniques are used (Fowler et al., 2007; Tang et al., 2016; Wilby & Wigley, 1997). Both techniques improve the models' prediction abilities on a regional scale. Regional climate models (RCMs) are used for dynamical downscaling to produce regional-scale simulations and projections for atmospheric variables driven by GCMs, such as temperature, rainfall, and wind (Rockel, 2015; Tang et al., 2016; Wang et al., 2004). Statistical downscaling, on the other hand, is used to predict a local climate variable (the predictands) from large-scale variables (the predictors) (Nageswararao et al., 2016a; Tang et al., 2016). The main advantage of statistical approaches is that they make less computational demand, but they require a long-term and high-quality observational dataset to establish the relationship between large- and regional-scale variables (Tang et al., 2016). So, one can use the dynamical model, which includes all sub-grid scale processes in the form of various numerical models and is too expensive to use dynamical downscaling outputs, i.e., RCM output, and improves its output by using statistical downscaling, which is a good combination a for regional study. The World Climate Research Program (WCRP) recently launched the coordinated regional climate downscaling experiment (CORDEX) project to improve global regional climate projections (Giorgi et al., 2009; Sannan et al., 2020). A study of all Indian summer monsoon rainfall found that CORDEX-SA needs to improve its driving GCMs to accurately simulate Indian summer monsoon rainfall (Choudhary et al., 2019).

The CORDEX-SA RCMs can simulate rainfall projections over the Himalayan region (Choudhary & Dimri, 2018). The Consortium for Small-Scale Modeling (COSMO) regional Climate Model (COSMO-CLM) is one of the CORDEX-SA RCMs that can capture semi-permanent systems such as the seasonal heat low, monsoon trough, Tibetan anticyclone, tropical easterly jet, low-level jet, or Somali jet over the Indian region during JJAS (Patwardhan et al., 2016). Sannan et al. (2020) used CORDEX-SA RCMs to simulate the northeast monsoon rainfall, also known as winter rainfall, which is a major rainy season in South Peninsular India. They discovered that CORDEX-SA RCMs could simulate the spatial distribution of northeast monsoon seasonal rainfall and its variability over Southern Peninsular India. Furthermore, the current set of CORDEX-SA RCM simulations provides value to their driving GCMs to improve Indian summer monsoon rainfall simulations, necessitating RCM re-evaluation (Choudhary et al., 2018). Observational data, as well as CORDEX-SA data, have been used in numerous studies on climate forecasts for the southwest monsoon and annual rainfall across India (Choudhary & Dimri, 2019; Dimri et al., 2018a, 2018b, 2019; Dobler & Ahrens, 2010; Kumar et al., 2011; Rajeevan & Nanjundiah, 2009; Sharmila et al., 2015); a detailed examination of RCM performance for ISMR over East India (EI) is carried out in this study, where summer monsoon rainfall has considerably declined in recent decades (Barde et al., 2020). The decrease in rainfall over the monsoon core zone is associated with a decline in seasonal rainfall for India as a whole. According to several studies, a reduction in rainfall causes frequent dryness in this region (Mallay et al., 2016; Nath et al., 2017; Barde et al., 2020). The Brahmaputra and Gangetic Basins in the Indo-Gangetic Plains are the most flood-prone areas, according to Bhatla et al. (2015), and this region is one of the world's largest plains formed by river systems, resulting in a reduction in summer monsoon rainfall, which influences agriculture, the hydrological cycle, and overall public health. Furthermore, this is one of India's dense forest areas.

Chaturvedi et al. (2012) stated that policy-relevant suggestions for the near- (2025) and medium-term (2050) periods are impossible because of a lack of regional model forecasts. Sarthi et al. (2016) offered CMIP3 and CMIP5 seasonal rainfall projections for the Indo-Gangetic Plains up to 2099, although with a coarser geographical resolution. CMIP5 multi-model ensemble for the Indo-Gangetic Plains with $0.5^\circ \times 0.5^\circ$ spatial resolution has also been released by Nath et al. (2017). The performance of the CORDEX-SA experiment's RCMs is being tested to check the simulation of seasonal rainfall over EI. This study is particularly important in the context of contributing to the CORDEX project's superior aimed local-scale impact studies. The details of the study region, observational and model datasets, and methods utilized in this study are described in Sect. 2, while Sect. 3 discusses the results and Sect. 4 provides a summary and conclusions.

2. *Data and Methodology*

2.1. *Study Area*

East India (EI) is divided into four subdivisions: Bihar (BH), Jharkhand (JH), Chhattisgarh (CH), and Odisha (OD), shown in Fig. 1. EI encompasses a substantial portion of India's dense forest. The climate of the forest area over a large part of CH and OD is variable; according to pollen records, the climate is dry and cold, and seasonal rainfall decreased from 12,785 to 9035 B.C.; after that, a warm and moderately humid climate was established over the forest area with increased seasonal rainfall (9035 to 4535 B.C.). Finally, a warm and highly humid climate was established with a further increase in seasonal rainfall (4535 B.C. to present) (Quamar & Bera, 2017). Bihar is located in northeastern India and is part of the Gangetic Plains, which have enriched with fertilized alluvial soil and plentiful water supplies. Rice is a 'Kharif' crop whose growing season coincides with the summer monsoon season and is grown in all of Bihar's districts (Tesfaye et al., 2017). Because rainfed agriculture covers > 80% of Jharkhand, seasonal rainfall fluctuation has a significant impact on food, water, and the economy (Dey & Sarkar, 2011). This study uses a combination of all four regions to understand changes in seasonal rainfall using RCM's future emissions.

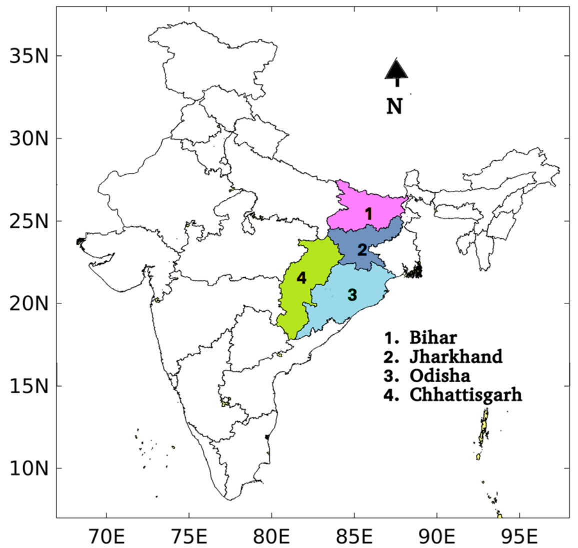

Figure 1
The study region of East India

2.2. *Observational and Model Dataset*

The India Meteorological Department's (IMD) high-resolution (0.25° × 0.25°) gridded daily rainfall analysis dataset is used for the period 1971–2005 to evaluate the performance of CORDEX-SA RCM rainfall data over EI. To prepare the IMD data set, 6955 rain gauge station records in India have been used. The density of stations is variable, and on average, 2600 stations have available records (Pai et al., 2014). Recent studies have shown that this dataset is most widely used for the assessment of RCMs in India (Pai et al., 2015; Barde et al., 2020; Nageswararao et al., 2016b; Sannan et al., 2020).

To produce better regional climate change projections over different domains of the world, the CORDEX project under the World Climate Research Program (WCRP) was developed (Giorgi et al., 2009; Sannan et al., 2020). The CORDEX is a coupled atmosphere-ocean general circulation model (AOGCM), which is taken from ten different RCM-GCM combinations arising from five RCMs forced with eight GCMs that come from CMIP5. The RCM's daily rainfall data for the CORDEX-SA experiment are available at the FTP server of the Center for Climate Change Research (CCCR), Indian Institute of Tropical Meteorology, Pune, India (http://cccr.tropmet.res.in/home/cordexsa_datasets.jsp). In this study, the JJAS rainfall from ten Regional Climate Models (RCMs) of the CORDEX-SA experiment is available at 0.4° spatial resolution (~ 50 km) for the period of 100 years (1971–2070). The availability of datasets from various RCMs are different, which is provided in Table 1. After 2005, in the simulations of RCMs, the forcing is generated based on the representative concentration pathway (RCP) scenarios (Moss et al., 2010; Sannan et al., 2020). Worldwide, RCP2.6, RCP4.5, RCP6, and RCP8.5 are used for future projections; the number for RCPs indicates the amount of radiative forcing by 2100 with + 2.6, + 4.5, + 6, and + 8.5 Watts per square meter (W/m^2), respectively (Slater & Lawrence, 2013). Previously, studies have used the fragment method for future projections to analyze the

Table 1

Details of data sets used in the study

Data name	Variable	Spatial resolution	Available time period	Institute
IMD observation	Rainfall	0.25° × 0.25°	1901–2016	India Meteorological Department
COSMO_CLM	Rainfall	0.4° × 0.4°	1951–2100	Institute for Atmospheric and Environmental Sciences (IAES), Goethe University, Frankfurt am Main (GUF), Germany
GFDL-ESM2M-IITM-RegCM4	Rainfall	0.4° × 0.4°	1951–2005	CCCR-IITM, Pune, India
LMDz-IITM-RecCM4	Rainfall	0.4° × 0.4°	1951–2005	CCCR-IITM, Pune, India
ACCESS-CSIRO-CCAM	Rainfall	0.4° × 0.4°	1971–2099	CSIRO Marine and Atmospheric Research, Melbourne, Australia
GFDL-CM3-CSIRO-CCAM	Rainfall	0.4° × 0.4°	1971–2099	CSIRO Marine and Atmospheric Research, Melbourne, Australia
CNRM-CM5-CSIRO-CCAM	Rainfall	0.4° × 0.4°	1971–2099	CSIRO Marine and Atmospheric Research, Melbourne, Australia
CCSM4-CSIRO-CCAM	Rainfall	0.4° × 0.4°	1971–2099	CSIRO Marine and Atmospheric Research, Melbourne, Australia
MPI-ESM-LR-CSIRO-CCAM	Rainfall	0.4° × 0.4°	1971–2099	CSIRO Marine and Atmospheric Research, Melbourne, Australia
MPI-ESM-LR-CSIRO-CCAM	Rainfall	0.4° × 0.4°	1971–2099	CSIRO Marine and Atmospheric Research, Melbourne, Australia
ICHEC-EC-EARTH-SMHI-RCA4	Rainfall	0.4° × 0.4°	1971–2099	Rossby Centre, Swedish Meteorological and Hydrological Institute (SMHI), Sweden

changes in the near and far future (Choudhary & Dimri, 2019; Dimri et al., 2018a, 2018b; Kumar & Dimri, 2018; Sannan et al., 2020). In this study, the common availability period of 35 years (1971–2005) as a hindcast (past) mode and 11 years (2006–2016) as the present period (validation period) and 2016–2040 and 2041–2070 as near and far future projection periods are considered, respectively.

2.3. Methodology

A total of ten RCMs have been used, ACCESS-CSIRO-CCAM (M1), GFDL-CM3-CSIRO-CCAM (M2), CNRM-CM5-CSIRO-CCA (M3), COSMO_CLM (M4), CCSM4-CSIRO-CCAM (M5), GFDL-ESM2M-IITM-RegCM4 (M6), ICHEC-EC-EARTH-SMHI-RCA4 (M7), LMDz-IITM-RecCM4 (M8), MPI-ESM-LR-CSIRO-CCAM (M9), and Nor-ESM1-M-CSIRO-CCAM (M10). The RCMs and observational dataset grid sizes differ, so the CORDEX-SA RCM's rainfall outputs are re-gridded to the observational grid (0.25° × 0.25°) points using a bilinear interpolation technique. To check the spatial pattern and performance of RCMs for ISMR over EI, climatological mean, inter-annual variability (IAV), coefficient of variation (CV), index of agreement (IOA), root mean square error (RMSE), and mean bias (MB) have been computed for each grid and sub-divisional level for the hindcast period (1971–2005). To remove the systematic bias present in the RCM outputs, linear scaling (LS) addition, LS multiplication, standardized reconstruction technique (SRT), and quantile mapping (QQM) are used (Acharya et al., 2013; Mohanty et al., 2019). The SRT bias correction method is used to eliminate the systematic error (algebraic mean difference) between observed and RCM data, and the QQM bias correction method is widely used to correct systematic distributional bias in GCMs and RCMs (Acharya et al., 2013; Ajaaj et al., 2016). The formulation of QQM is as follows,

$$F_i = CDF_{ob}^{-1}(CDF_M(Xm(t))) \tag{1}$$

CDF_{ob}^{-1} is the inverse cumulative distribution function for observed data, CDF_M is the cumulative distribution function for RCMs, and Xm is the RCM data. To maintain the pattern of RCPs after bias correction, the difference value of PDF F_i^D between future projection PDF (F_i^f) and hindcast mode RCMs (F_i) is added to bias-corrected future projection PDF.

$$F_i^D = F_i^f - F_i \quad (2)$$

F_i is the bias-corrected RCMs hindcast quantile data, and F_i^f is RCM's future projection quantile.

Only models that have both RCPs available, i.e., RCP 4.5 and RCP 8.5, are used for future projection analysis. Among all RCMs, only six have both RCPs; M1, M2, M3, M7, M9, and M10 have been used. The probability density function (PDF) method has been used to compare raw and bias-corrected data. The leave-one-out cross-validation procedure is used to generate bias-corrected data for the present period. The corrected data are used for future projection analysis. Changes in the percentage of rainfall for the concerned current period (1971–2005) are also checked to understand rainfall distribution in the future (Sannan et al., 2020).

3. *Results and Discussion*

The spatial pattern of JJAS seasonal rainfall over EI is analyzed to check RCM's ability to reproduce the seasonal rainfall in terms of long-term mean, IAV, and CV. Next, RCM's ability to simulate the temporal variation of seasonal rainfall has been analyzed. Furthermore, the spread of each model, long-term mean, IAV, and mean bias has been calculated for EI as a whole and its four subdivisions. Finally, a time series and spatial pattern are used to determine the change in JJAS seasonal rainfall over EI for up to the year 2070, and the bias-corrected seasonal rainfall projections are used to identify the probable deficit and excess rainfall years in the near and far future for two RCP scenarios.

3.1. *Spatial Pattern of JJAS Seasonal Rainfall over EI by Using CORDEX-SA RCMs*

The performance of ten CORDEX-SA RCMs in reproducing JJAS seasonal mean rainfall over EI from 1971 to 2005 is shown in Fig. 2. Because it is a part of the monsoon core zone, the JJAS mean seasonal rainfall from IMD is > 700 mm, and maximum rainfall is observed over the central and south parts of EI (Fig. 2a), i.e., Chhattisgarh, Odisha, and Jharkhand, while relatively less JJAS seasonal rainfall is observed over the north part, i.e., Bihar (Barde et al., 2020; Meshram et al., 2017; Sharma & Singh, 2017; Swain et al., 2018; Warwade et al., 2018). Notably, the RCMs developed by the CSIRO group, including M1, M2, M3, M9, and M10, may simulate a similar pattern to IMD but underestimate the magnitude of the JJAS seasonal rainfall. The M4, M6, M7, and M8 models, on the other hand, have large wet bais over EI's northern and eastern parts. Figure 3 shows that the IAV of JJAS rainfall from IMD is high over central EI, i.e., west Odisha, and some pockets of north and south EI, and it ranges from 500 to 550 mm. Notably, the region that shows a higher amount of seasonal rainfall also shows more variability from IMD. Similar to climatology, IAV is also high for M4 and M7. The M7 can capture the spatial pattern of IAV of seasonal rainfall but cannot precisely capture the magnitude.

The CSIRO group's RCMs, i.e., M1 (ACCESS-CSIRO-CCAM), M2 (GFDL-CM3-CSIRO-CCAM), M3 (CNRM-CM5-CSIRO-CCAM), M5 (CCSM4-CSIRO-CCAM), M9 (MPI-ESM-LR-CSIRO-CCAM), and M10 (NorESM1-M-CSIRO-CCAM), show higher IAV over south instead of central EI. On the other hand, IITM-RCMs, i.e., M6 (GFDL-ESM2M-IITM-RegCM4) and M8 (LMDz-IITM-RecCM4), have higher IAV over east EI. M4 shows high IAV over east and north EI, which is uncommon in other RCMs, and M7 shows high IAV over north EI (Fig. 3). The spatial pattern of seasonal rainfall of CV (%) indicates that the all CSIRO group's RCMs and M4 show higher CV for the southern part of EI (Fig. 4). Model M7 can capture the pattern of the CV but cannot capture the magnitude. Model M8 shows a higher CV for west EI which is not present at any other RCMs. M4 also shows a patch of high CV over central Odisha.

The CSIRO group's RCMs can simulate the climatological features of JJAS seasonal rainfall patterns across the southern part of EI based on the aforementioned study, but they lack in magnitude, which may be improved by adopting the appropriate bias correction approach. M4 and M7 accurately

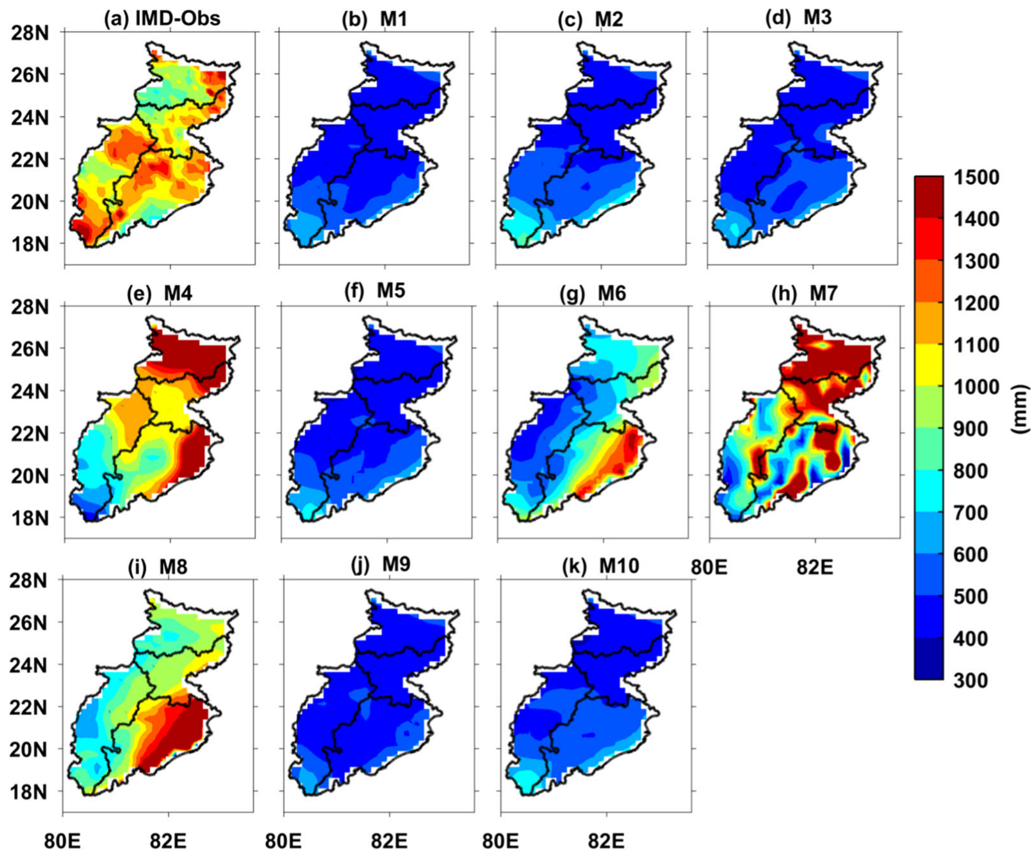

Figure 2

Spatial distribution of southwest summer monsoon (JJAS) rainfall (mm) from **a** India Meteorological Department (IMD) observation and ten regional climate model (RCMs) participating in the CORDEX_SA experiment such as **b** M1-ACCESS-CSIRO-CCAM, **c** M2-GFDL-CM3-CSIRO-CCAM, **d** M3-CNRM-CM5-CSIRO-CCAM, **e** M4COSMO-CLM, **f** M5-CCSM4CSIRO-CCAM, **g** M6-GFDL-ESM2M-IITM-RegCM4, **h** M7-ICHEC-EC-EARTH-SMHI-RCA4, **i** M8-LMDz-IITM-RecCM4, **j** M9-MPI-ESM-LR-CSIRO-CCAM, and **k** M10-NorESM1-M-CSIRO-CCAM over EI during the common period for all RCMs, 1971–2005

simulated rainfall in the northern portion of EI, whereas M7 can accurately simulate seasonal rainfall in most of EI except the southern section. The discrepancy of various RCMs in simulating the magnitude and pattern of seasonal rainfall is related to uncertainties present when GCMs are dynamically downscaled (Ebert & McBride, 2000; Sannan et al., 2020; Wehner et al., 2010).

3.2. Temporal Analysis of Seasonal Rainfall by Using CORDEX-SA RCMs over EI

Figure 5 depicts the year-to-year variation in the EI JJAS seasonal rainfall. The CSIRO group's RCMs produce very little rainfall over EI compared to IMD observed rainfall; IITM-RCMs, M4, and M7 produce reasonable rainfall over EI similar to IMD observed rainfall. In 1980, 1994, and 2001, observed JJAS seasonal rainfall is > 1200 mm. However, rainfall values from the CSIRO group's RCMs (400–800 mm) indicate a large dry bias in the model rainfall while other RCMs have a wet bias (1000–1400 mm). These results are also reflected in box plots of seasonal rainfall distribution for EI and its subdivisions, which have been plotted to illustrate the spread of observational and RCM rainfall datasets (Fig. 6). For EI, all CSIRO group's RCMs are spread in between 300 and 500 mm with a median of about 500 mm; however, observation is spread from 800–1400 mm with a median around 1080 mm. Model M7 shows a spread between 900 and 1400 mm, M8 shows a spread between 650 and

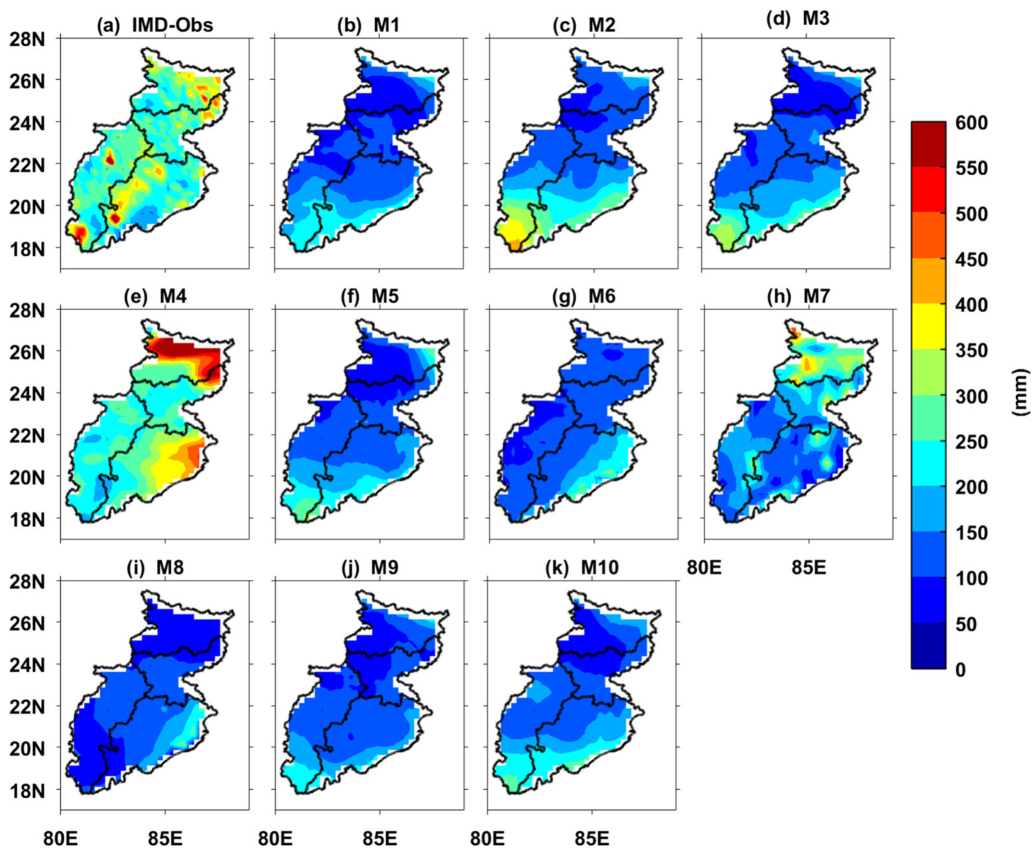

Figure 3
Same as Fig. 2 but for interannual variability (IAV) of JJAS rainfall

1350 mm, and M4 shows a spread between 900 and 1450 mm; these three RCM medians are closer to observation over EI (Fig. 6). The M4 and M7 show wet bias for all of EI, Bihar, Jharkhand, and Odisha, while all RCMs show dry bias for Chhattisgarh. Table 2 shows the multiplicative bias for RCMs; the efficiency of the model to simulate the climatology of rainfall is more when it is close to 1, and particularly M7 has more efficiency (1.095) followed by M8 (0.925), M4 (1.137), and M6 (0.702) while other RCMs' efficiency is < 0.5.

3.3. *Performance Evaluation of Raw and Bias-Corrected CORDEX-SA for EI JJAS Rainfall at Sub-divisional Level*

The performance of raw and bias-corrected RCMs in simulating JJAS seasonal rainfall over EI has been evaluated, and the results are discussed in this section. Analysis of the previous sections shows that the CSIRO group's RCMs are underestimating the JJAS seasonal rainfall over EI while the overestimation is noticed in the other RCMs. So, it is necessary to remove the systematic bias presented in the model by using an appropriate bias correction technique before projecting the future. The LS addition, LS multiplication, SRT, and QQM have been applied to improve the RCM rainfall output for the period 1971–2005 with leave-one-out cross-validation (LOOCV) approach and its performance evaluated against IMD observation. The detailed analysis of four bias correction techniques used in this study is presented in Table 3. RCM's JJAS seasonal rainfall outputs are significantly improved for all four bias correction methods. The climatological mean bias is completely reduced when LS addition and LS multiplication techniques are applied, but the difference in IAV between observation and model is too

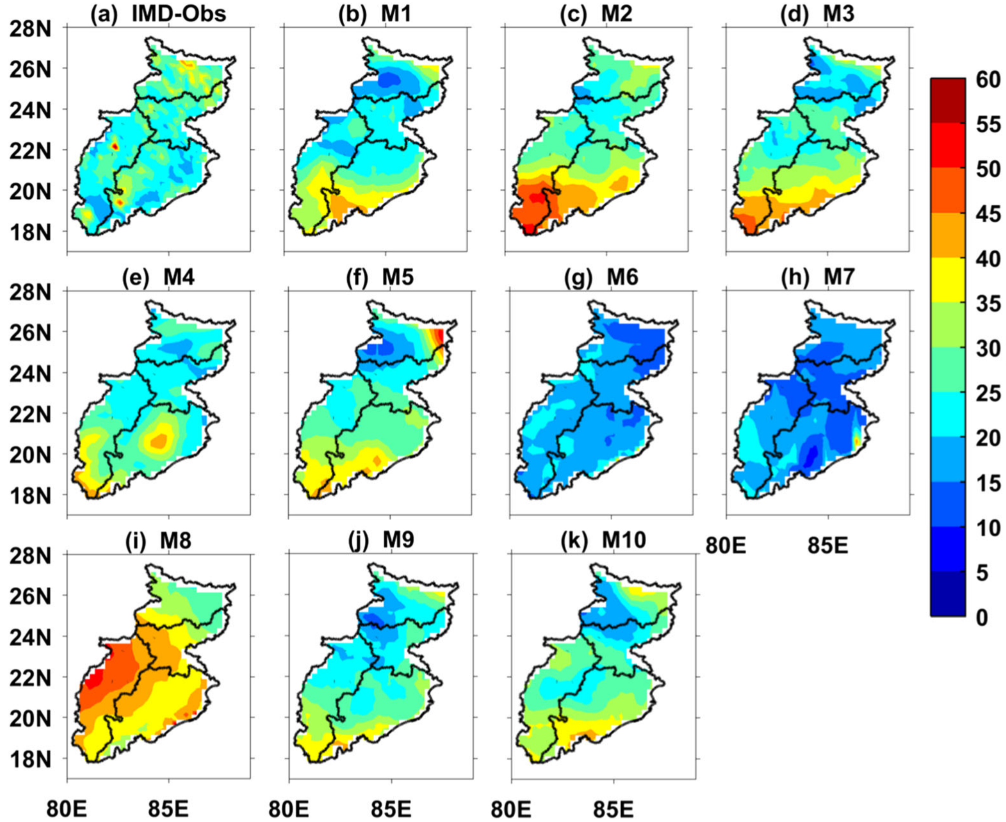

Figure 4
Same as Fig. 2 but for coefficient of variation (CV in %) of JJAS rainfall

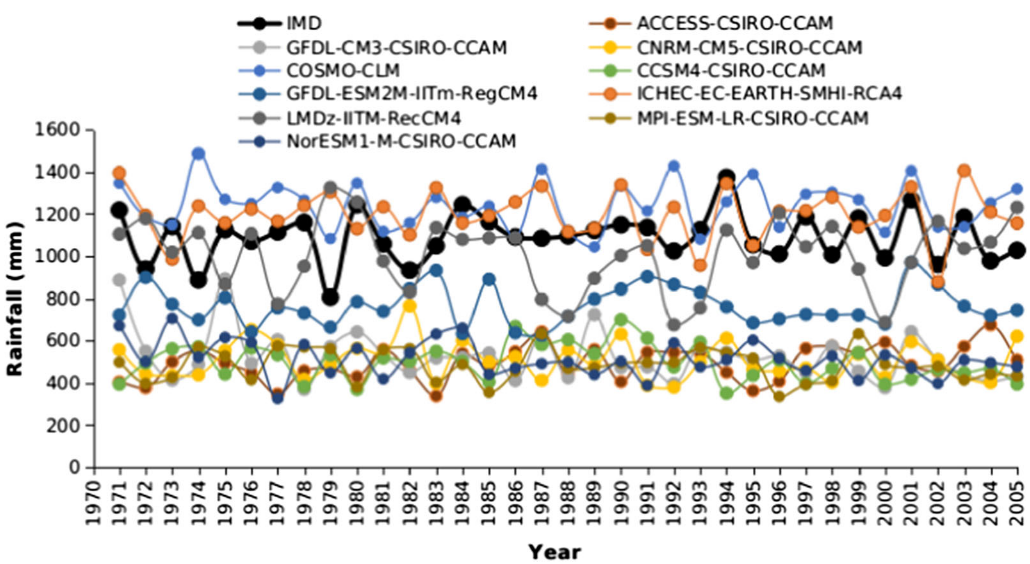

Figure 5
Year-to-year variation in the EI JJAS rainfall from IMD observation and regional climate model (RCMs) participating in the CORDEX_SA experiment for the period 1971–2005

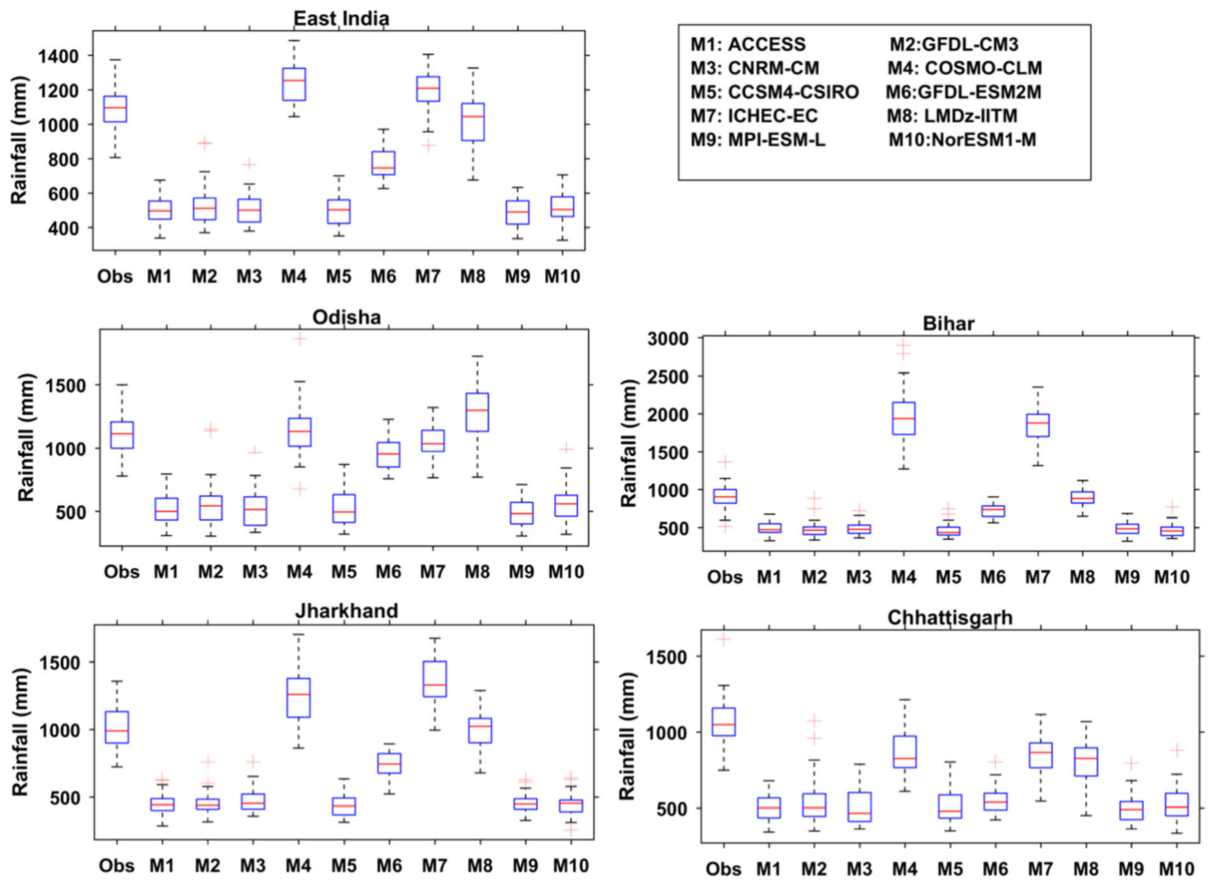

Figure 6

Box plot for the degree of spread of JJAS rainfall (mm) over EI from IMD observation and ten CORDEX-SA RCMs for the period 1971–2005. The centerline for each box represents the median value of the EI JJAS rainfall, while the bottom and top edges of the box represent the 25th and 75th percentile value of JJAS rainfall, and the '+' symbol represents the outliers of the data

Table 2

Multiplicative bias (RCMs climatology/observed climatology)

Regional climate model	Efficiency
ACCESS-CSIRO-CCAM	0.452
GFDL-CM3-CSIRO-CCAM	0.483
CNRM-CM5-CSIRO-CCAM	0.464
COSMO-CLM	**1.137**
CCSM4-CSIRO-CCAM	0.455
GFDL-ESM2M-IITM-RegCM4	**0.702**
ICHEC-EC-EARTH-SMHI-RCA4	**1.095**
LMDz-IITM-RecCM4	**0.925**
MPI-ESM-LR-CSIRO-CCAM	0.443
NorESM1-M-CSIRO-CCAM	0.471

The efficiency >1 (bold) indicates the wet bias in the model while the efficiency < 1 represents the dry bias in the model

large for some RCMs; for example, all RCMs show large IAV even after bias correction by using these two methods as compared to the observation except COSMO_CLM (LS addition: 117 mm, LS multiplication: 103 mm) and ICHEC-EC-EARTH-SMHI-RCA4 (LS addition: 124 mm, LS multiplication: 113 mm). The SRT and QQM methods are more reliable as they improve the mean bias, IAV, CV, and IOA (Table 3) and find QQM is a relatively better skill than the SRT (Acharya et al., 2013).

Figure 7 shows the diagnostic plot for JJAS summer monsoonal rainfall from ten RCMs. Seasonal rainfall from IMD observation is plotted against the seasonal rainfall from CORDEX-SA RCMs for the hindcast period. This method was previously used to check CORDEX RCM's performance over the monsoon core region of India (Choudhary et al., 2018). The raw data are shown in the black scatter plot (Fig. 7a), and bias-corrected data are shown in the

Table 3

Performance of various bias correction methods on RCMs for All India JJAS Rainfall over East India (EI) with standard skill metrics such as climatological mean (CLM), Interannual variability (IAV), coefficient of variation (CV), and index of agreement (IOA) against IMD observation for the period 1971–2005

RCMs	CLM (mm) Obs = 1091		IAV (mm) Obs = 116		CV (%) Obs = 10.6		Index of agreement (IOA)	
	Before	After	Before	After	Before	After	Before	After
Linear scaling: addition								
Rf_cor = Rf_M + Bt								
Bt = clm(O)-clm(M)								
ACCESS-CSIRO-CCAM	493	1091	81	84	16.4	7.7	0.22	0.32
GFDL-CM3-CSIRO-CCAM	527	1091	122	125	23.2	11.4	0.24	0.49
CNRM-CM5-CSIRO-CCAM	506	1091	90	92	17.8	8.4	0.23	0.54
COSMO-CLM	1240	1091	114	117	9.2	10.7	0.42	0.49
CCSM4-CSIRO-CCAM	497	1091	87	90	17.4	8.3	0.22	0.21
GFDL-ESM2M-IITM-RegCM4	766	1091	90	92	11.8	8.5	0.32	0.45
ICHEC-EC-EARTH-SMHI-RCA4	1196	1091	121	124	10.1	11.3	0.48	0.48
LMDz-IITM-RecCM4	1010	1091	167	172	16.5	15.7	0.26	0.33
MPI-ESM-LR-CSIRO-CCAM	484	1091	75	78	15.6	8.0	0.21	0.34
NorESM1-M-CSIRO-CCAM	514	1091	85	87	16.5	7.1	0.23	0.41
Linear scaling: multiplicative bias								
Rf_cor = Rf_M × (clm(O)/clm(M))								
ACCESS-CSIRO-CCAM	493	1092	81	185	16.4	16.9	0.22	0.31
GFDL-CM3-CSIRO-CCAM	527	1093	122	262	23.2	24.0	0.24	0.40
CNRM-CM5-CSIRO-CCAM	506	1092	90	200	17.8	18.3	0.23	0.51
COSMO-CLM	1240	1091	114	103	9.2	9.4	0.42	0.48
CCSM4-CSIRO-CCAM	497	1092	87	197	17.4	18.0	0.22	0.20
GFDL-ESM2M-IITM-RegCM4	766	1092	90	132	11.8	12.1	0.32	0.46
ICHEC-EC-EARTH-SMHI-RCA4	1196	1092	121	113	10.1	10.3	0.48	0.48
LMDz-IITM-RecCM4	1010	1092	167	186	16.5	17.0	0.26	0.32
MPI-ESM-LR-CSIRO-CCAM	484	1092	75	176	15.6	16.1	0.21	0.35
NorESM1-M-CSIRO-CCAM	514	1092	85	186	16.5	17	0.23	0.40
Standardized reconstruction technique								
Mt = (Mi-clm(M))/σ_M								
Rf_corr = Mt × σ_O + clm(O)								
ACCESS-CSIRO-CCAM	493	1092	81	123	16.4	11.3	0.22	0.31
GFDL-CM3-CSIRO-CCAM	527	1094	122	129	23.2	11.8	0.24	0.45
CNRM-CM5-CSIRO-CCAM	527	1094	122	129	23.2	11.8	0.23	0.50
COSMO-CLM	1240	1092	114	121	9.2	11.1	0.42	0.45
CCSM4-CSIRO-CCAM	506	1092	90	123	17.8	11.3	0.22	0.21
GFDL-ESM2M-IITM-RegCM4	1240	1092	114	121	9.2	11.1	0.32	0.43
ICHEC-EC-EARTH-SMHI-RCA4	497	1093	87	123	17.4	11.3	0.48	0.46
LMDz-IITM-RecCM4	766	1092	90	122	11.8	11.1	0.26	0.32
MPI-ESM-LR-CSIRO-CCAM	1196	1089	121	123	10.1	11.3	0.21	0.34
NorESM1-M-CSIRO-CCAM	1010	1089	167	122	16.5	11.2	0.23	0.40
Quantile–quantile mapping								
ACCESS-CSIRO-CCAM	484	1091	75	122	15.6	11.2	0.22	0.31
GFDL-CM3-CSIRO-CCAM	514	1092	85	123	16.5	11.3	0.24	0.46
CNRM-CM5-CSIRO-CCAM	493	1092	81	124	16.4	11.3	0.23	0.51
COSMO-CLM	527	1094	122	134	23.2	12.3	0.42	0.46
CCSM4-CSIRO-CCAM	506	1092	90	126	17.8	11.5	0.22	0.21
GFDL-ESM2M-IITM-RegCM4	1240	1092	114	122	9.2	11.2	0.32	0.44
ICHEC-EC-EARTH-SMHI-RCA4	497	1093	87	125	17.4	11.4	0.48	0.47
LMDz-IITM-RecCM4	766	1093	90	124	11.8	11.4	0.26	0.33
MPI-ESM-LR-CSIRO-CCAM	1196	1090	121	121	10.1	11.1	0.21	0.35
NorESM1-M-CSIRO-CCAM	1010	1089	167	121	16.5	11.1	0.23	0.40

blue scatter plot (Fig. 7b). Correlation values of 0.41, 0.34, 0.32, and 0.31 for RCMs M9, M1, M10, M5, and M8, respectively, show the highest performance for raw data (Fig. 6a). The QQM method shows slight improvement in prediction skill compared to other methods; M9 (0.54) and M3 (0.45) have shown the highest performance, followed by M1(0.37), M10 (0.35), M5 (0.34), and M2 (0.33), respectively (Fig. 7b).

The long-term JJAS mean rainfall of EI and its subdivisions for the period 1971–2005 by RCM raw data (thick bar) and their bias-corrected outputs (thin bars) and the observed value of rainfall (red line) are presented in Fig. 8a. For simplification of plotting, RCMs are numbered from 1 to 10. The observed seasonal JJAS mean rainfall for the period 1971–2005 is 290, 570, 990, 610, and 1080 mm for BH, CH, JH, OD, and EI, respectively. All RCMs show overestimated JJAS mean seasonal rainfall for BH. Also, RCMs M4, M6, M7, and M8 overestimate the rainfall for all four subdivisions as well as EI as a whole. In comparison, the remaining RCMs underestimate the rainfall for EI and its subdivisions, and this analysis supports the analysis of Fig. 1. The long-

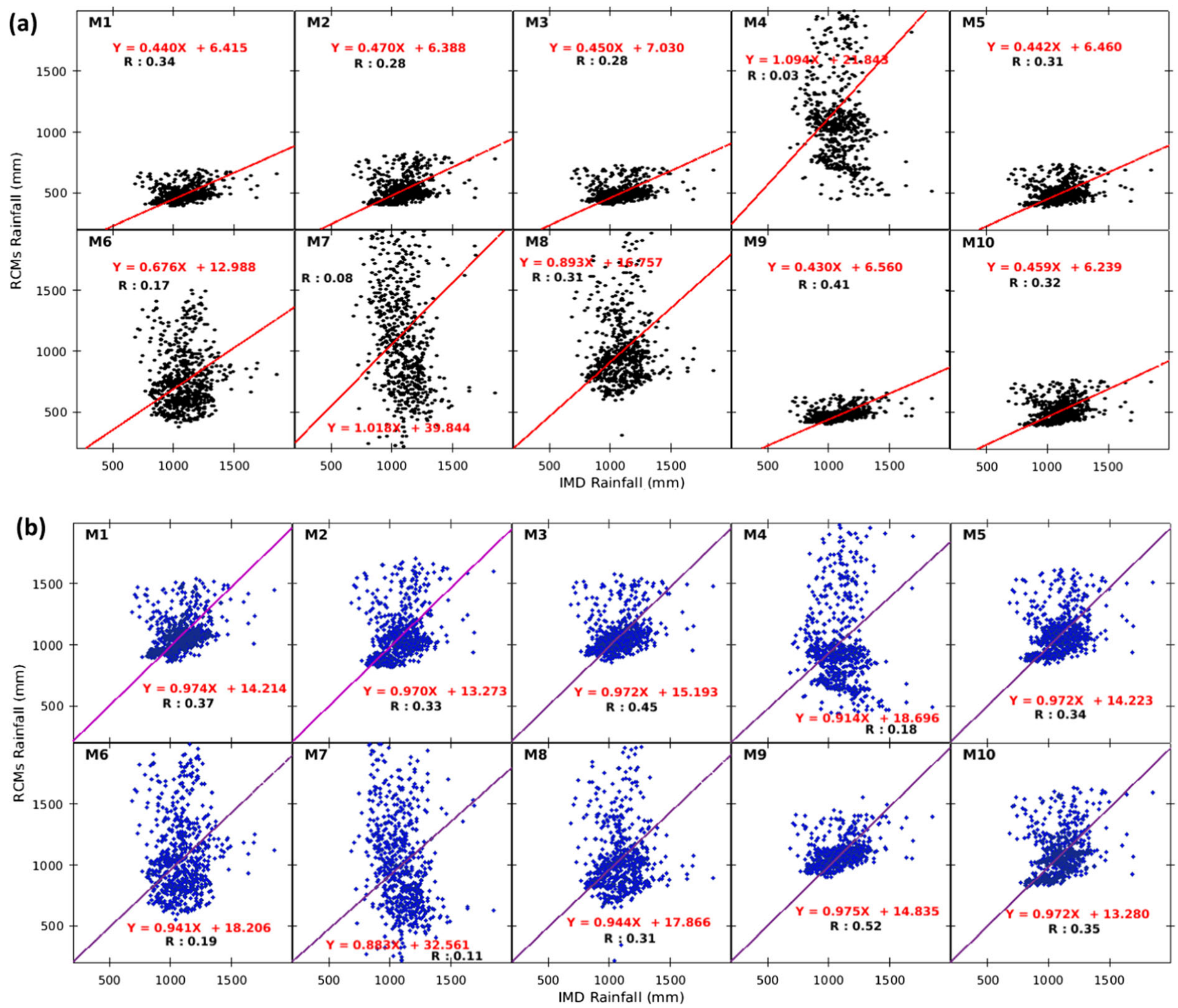

Figure 7

Diagnostic plot for JJAS rainfall (mm) from ten CORDEX-SA RCMs for hindcast period (1971–2005). **a** Raw and **b** bias-corrected RCMs against IMD observation. The black and blue color dots represent raw and bias-corrected RCM outputs and R indicates the correction coefficient values

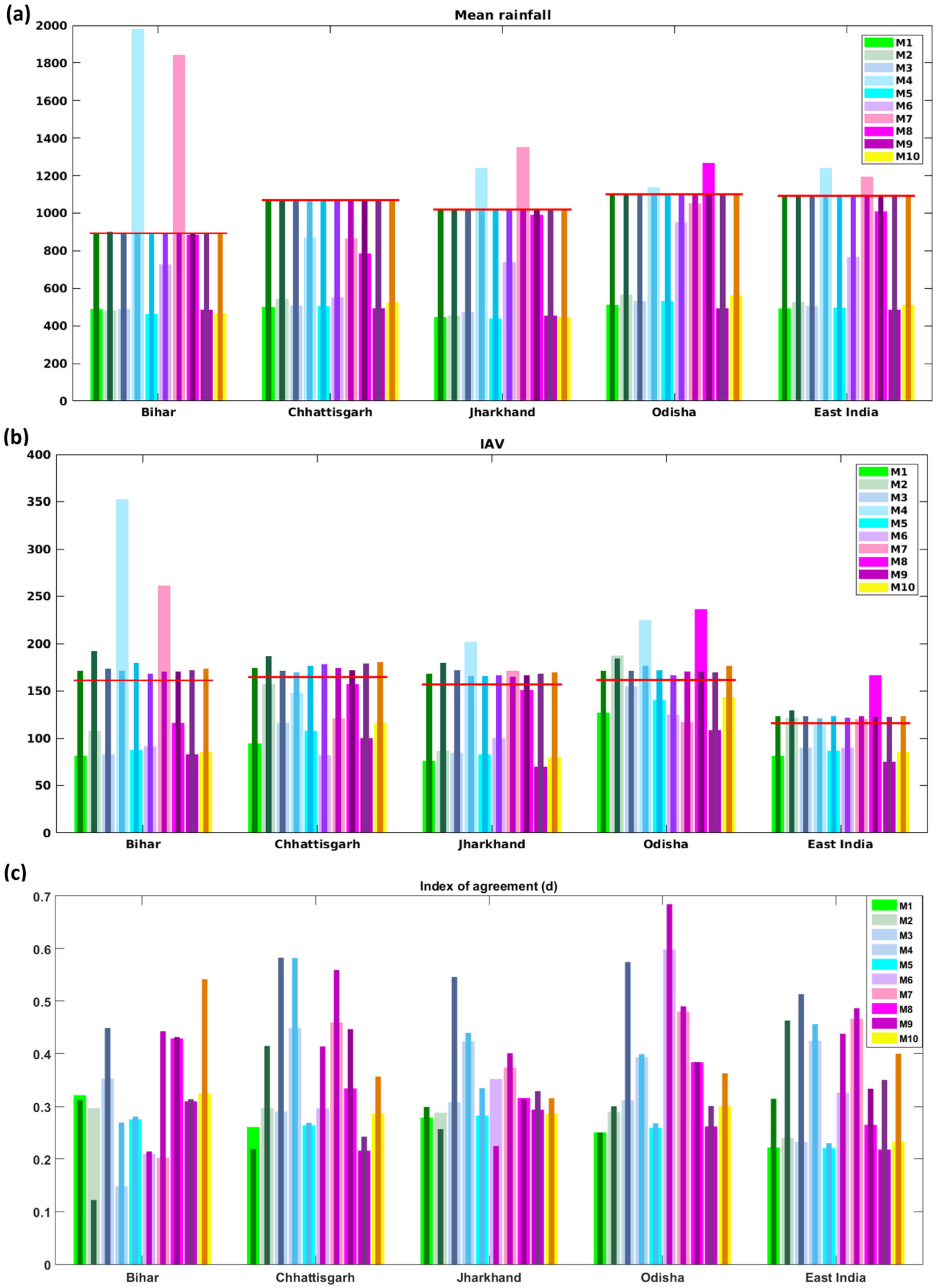
(a)
Mean rainfall
0
200
400
600
800
1000
1200
1400
1600
1800
2000
Bihar
Chhattisgarh
Jharkhand
Odisha
East India
M1
M2
M3
M4
M5
M6
M7
M8
M9
M10
(b)
IAV
0
50
100
150
200
250
300
350
400
Bihar
Chhattisgarh
Jharkhand
Odisha
East India
M1
M2
M3
M4
M5
M6
M7
M8
M9
M10
(c)
Index of agreement (d)
0
0.1
0.2
0.3
0.4
0.5
0.6
0.7
Bihar
Chhattisgarh
Jharkhand
Odisha
East India
M1
M2
M3
M4
M5
M6
M7
M8
M9
M10

◀ Figure 8
Subdivision-wise statistical skill scores of CORDEX-SA regional climate models in simulating the JJAS rainfall over EI for the period 1971–2005. **a** Climatological mean (mm), **b** inter-annual variability (IAV in mm), **c** index of agreement, **d** root mean square error (RMSE), and **e** mean bias. The light and dark color bars indicate the raw data and bias-corrected CORDEX-SA RCM outputs, and the horizontal line indicates IMD observation

term mean of JJAS rainfall from all the bias-corrected RCMs for all four subdivisions and EI as a whole is very close to the reality compared with the raw RCMs.

The IAV of seasonal rainfall from IMD observation is 120 mm for EI, 49 mm over BH, 110 mm over CH, 156 mm over JH, and 114 mm for Odisha for 1971–2005 (Fig. 8b). Similar to the climatological

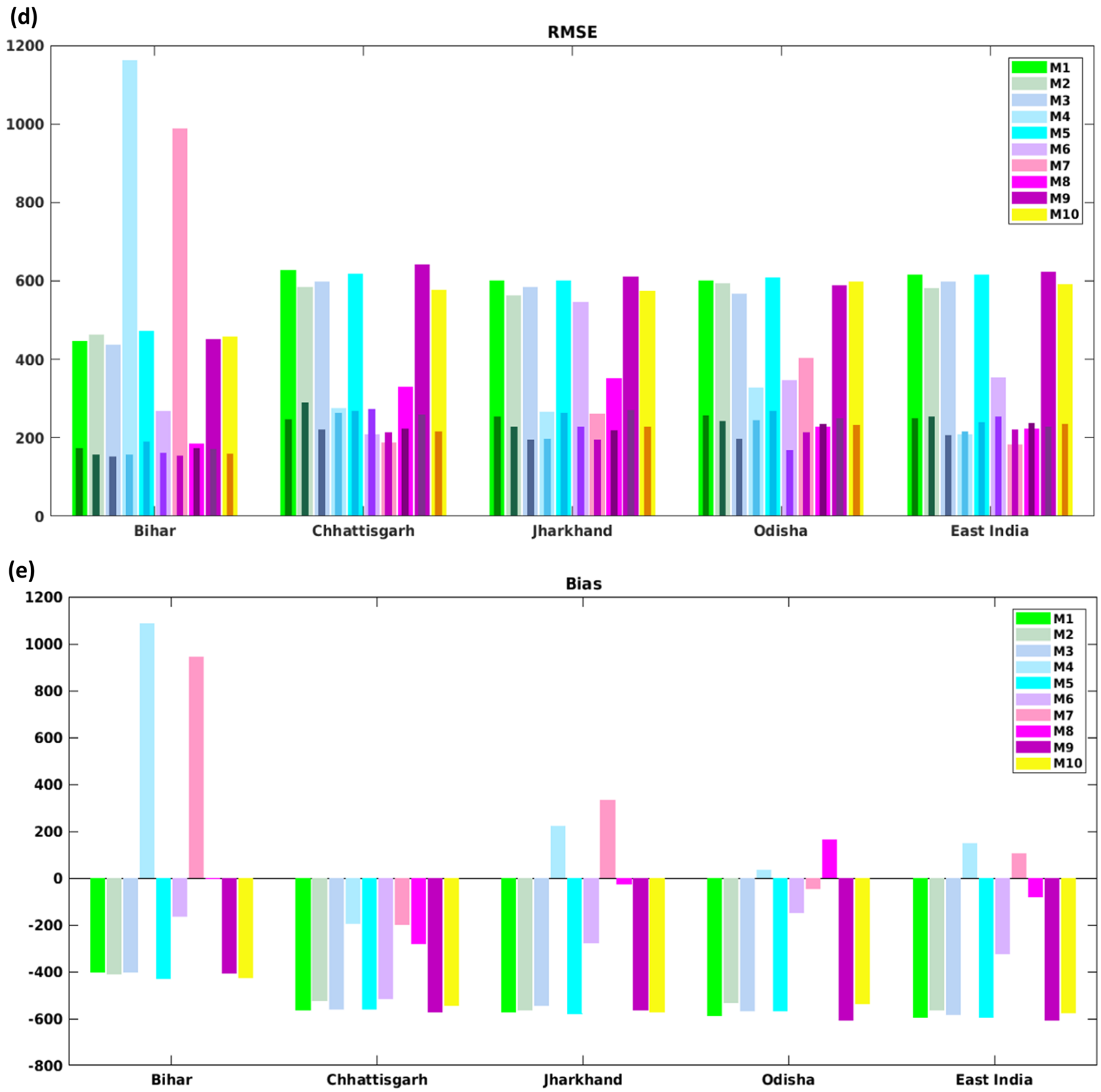

Figure 8
continued

mean, M7 shows the large overestimation of IAV for BH and JH before bias correction while all the model's IAV is underestimated for all subdivisions. After bias correction, all RCM's IAV is very close to the IMD observation for all sub-divisions and EI (Fig. 8b). RCM M6, M7, and M8 models agreed better with IMD observation than other models. After bias correction, all models show that the index of agreement (IOA) is near 0.5 (Fig. 8c). RMSE provides a measure of data accuracy in terms of how closely data spread around the mean value. The good data show lower RMSE value, and RMSE after bias correction is less than before (Fig. 8d). Furthermore, mean bias analysis shows a significant improvement (Fig. 8e).

3.4. Future Projections of Seasonal Rainfall over EI

For checking the future rainfall projections, the probability density function (PDF) has been prepared only for a few RCMs with both RCP4.5 and RCP 8.5 datasets, i.e., M1(ACCESS-CSIRO-CCAM), M2 (CNRM-CM5-CSIRO-CCAM), M3 (GFDL-CM3-CSIRO-CCAM), M7 (ICHEC-EC-EARTH-SMHI-RCA4), M9 (MPI-ESM-LR-CSIRO-CCAM), and M10 (NorESM1-M-CSIRO-CCAM). The model COSMO_CLM is good for most cases, but it has only an RCP4.5 projection, so it is not considered (Fig. 9). Considering the improvement in RCM output, an enhancement in the performance of the yearly forecast is expected and is highly required for policymaking, agriculture, and water management over EI.

The raw data PDF for the hindcast period and future projection are shown in Fig. 8a. In raw data, the mean seasonal rainfall for future projections from both RCPs is close to the hindcast period for M1, M2, M3, and M10. The shape and variability differ from RCM to RCM. Future distribution obtained by the QQM bias correction method to RCM simulations is shown in Fig. 8b. Bias-corrected seasonal rainfall for the hindcast period resembles the shape and mean value of the observation PDF. A small difference in variability is observed for M2, M7, M9, and M10. The seasonal variability, mean, and shape of bias-corrected data of M1 are closer to IMD observational data than other RCMs.

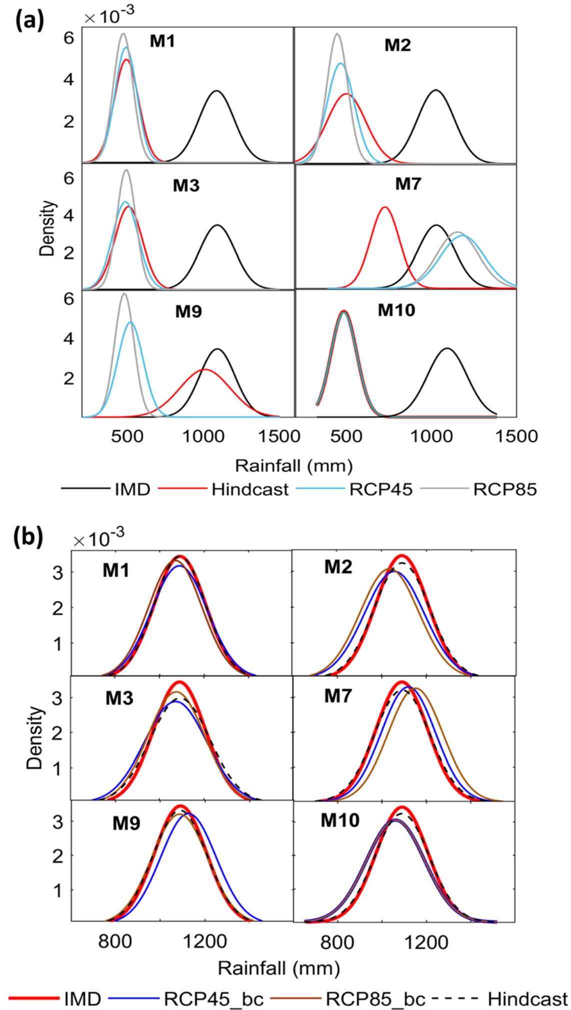

Figure 9
Probability distribution function (PDF) of JJAS rainfall over EI from **a** raw and **b** bias-corrected (QQ mapping) selected six CORDEX-SA RCM outputs against IMD observation for hindcast (1971–2005), near (2017–2040) and far future (2041–2070) time periods with RCP4.5 and RCP 8.5 emission scenarios (RCMs having both RCPs are only considered for future projection analysis, **M1**: ACCESS-CSIRO-CCAM, **M2**: GFDL-CM3-CSIRO-CCAM, **M3**: CNRM-CM5-CSIRO-CCAM, **M4**: COSMO-CLM, **M5**: CCSM4CSIRO-CCAM, **M6**: GFDL-ESM2M-IITM-RegCM4, **M7**: ICHEC-EC-EARTH-SMHI-RCA4, **M8**: LMDz-IITM-RecCM4, **M9**: MPI-ESM-LR-CSIRO-CCAM and **M10**: NorESM1-M-CSIRO-CCAM)

Figure 9 shows the time series of seasonal rainfall of EI by using raw RCM data (yellow color) and bias-corrected data (light blue color) for the period 2005–2070. In Figs. 10 and 11, the black line shows the control/current period observation. The bias-corrected data show good agreement with IMD

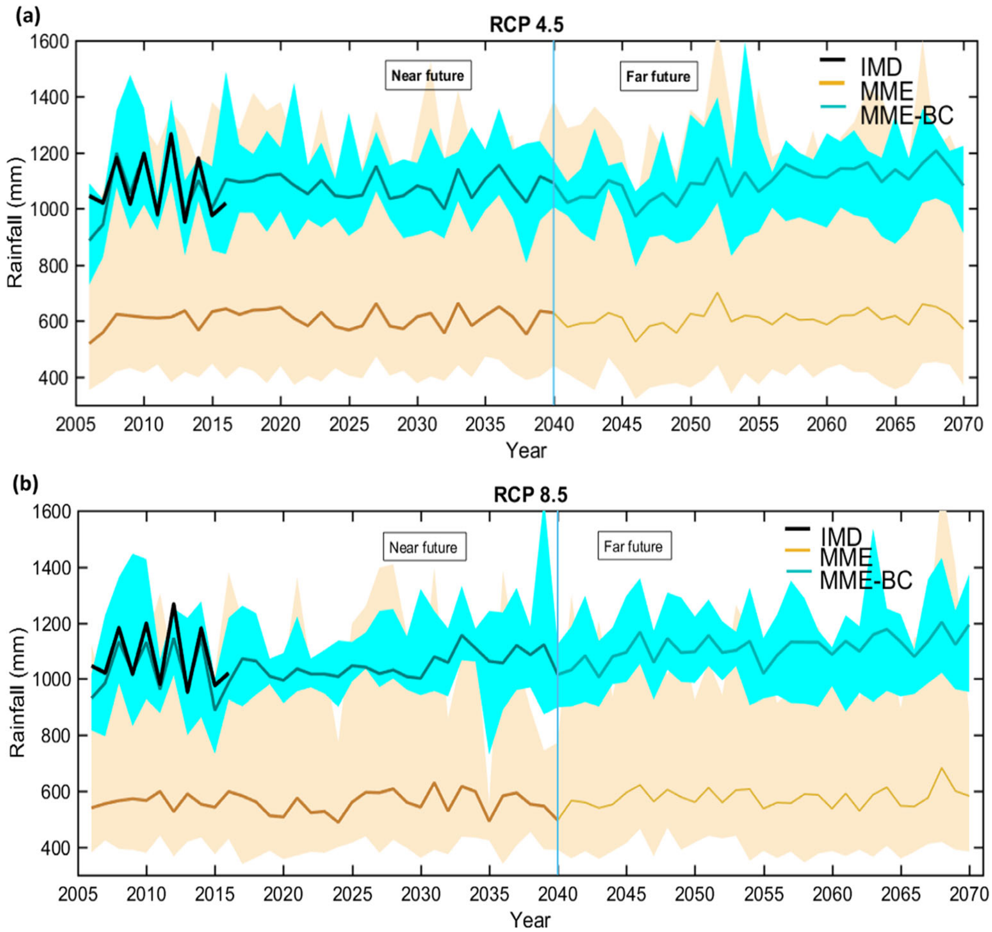

Figure 10
Future projections of JJAS rainfall from the mean of six raw and bias-corrected selected CORDEX-SA RCMs over EI with different emission scenarios: **a** RCP4.5 and **b** RCP8.5 for the period 2006–2070. The black line shows the IMD observation, the brown line shows the multi-model ensemble (MME) for raw data, and the blue line shows the MME for bias-corrected data

observation for the current period. Therefore, it is assumed that the projections calculated from these bias-corrected data show a good representation of future climate over EI (Fig. 10). The standardized anomaly of RCP 4.5 indicates the JJAS seasonal rainfall decreased for the near future and increased for the far future; the same information is getting by 5-year moving means (Fig. 11a). The 5 deficit rainfall years are projected for the near future, while only 2 deficit years are projected for the far future. RCP4.5 and RCP 8.5 also show good agreement with IMD observation for the present period (Fig. 10b). Interestingly, more excess rainfall years are projected for the far future as compared to the near future. Only 4 excess rainfall years are projected in the near future, while 6 excess rainfall years for the far future (Fig. 11b). So, the rainfall amount must be increased in the far future compared to the near future.

The projected changes in mean seasonal rainfall from CORDEX-SA RCMs and ensemble means relative to the hindcast period 1971–2005 for the near future and far future under RCP4.5 and RCP8.5 scenarios are shown in Figs. 12 and 13, respectively. The remarkable change in the JJAS seasonal rainfall is projected in the RCP 4.5 scenario. The reduction in JJAS seasonal rainfall is projected over the southern and eastern parts of EI (Chhattisgarh and Odisha) and enhanced rainfall projected over EI’s north and west parts by all RCMs for the near future (Fig. 12a). However, the same pattern is observed by most of

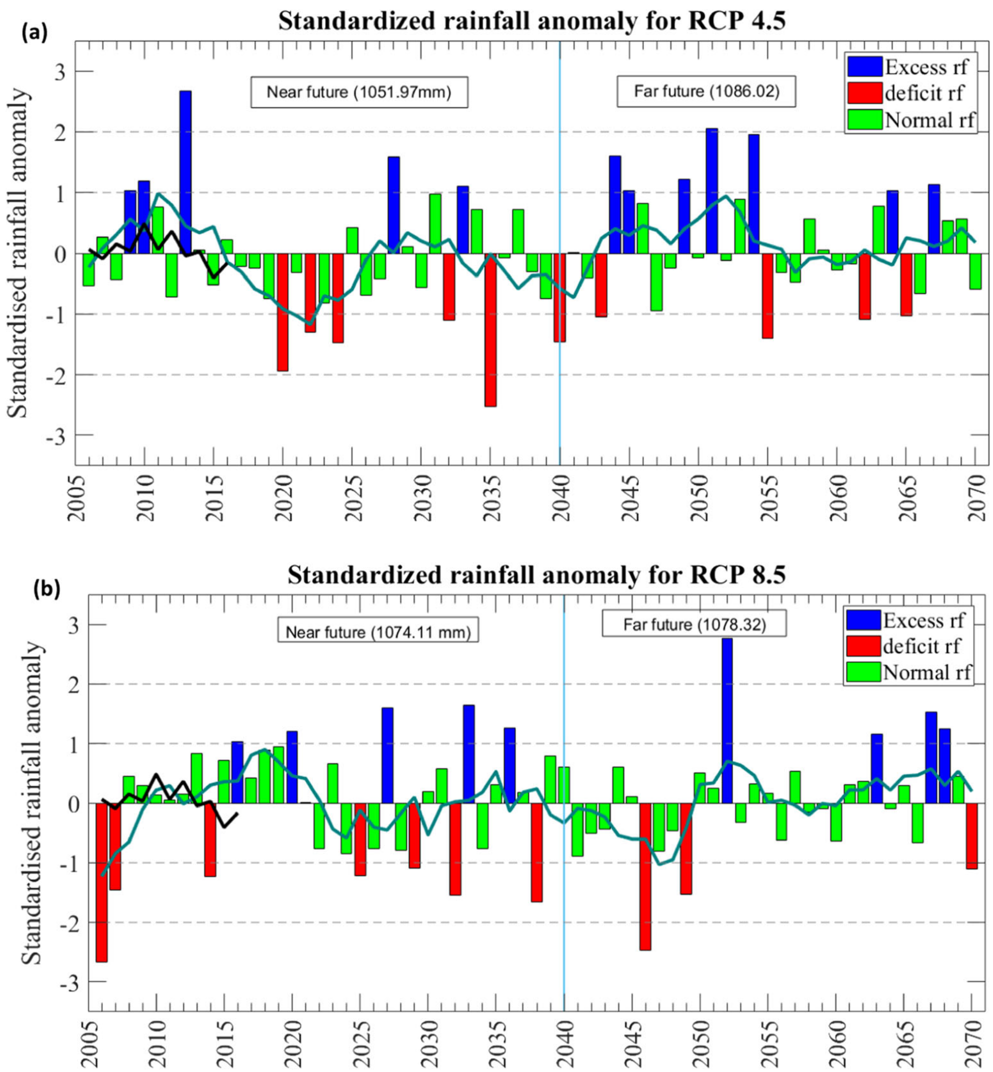

Figure 11
Standardized anomaly of future JJAS rainfall over EI based on present climate (1971–2005) with different scenarios. **a** RCP4.5, **b** RCP8.5 from the mean of six selected bias-corrected CORDEX-SA RCMs. The dark green and black lines indicate a 5-year running mean from six selected bias-corrected CORDEX-SA RCMs mean and IMD observation, respectively

RCMs for the far future except ICHEC-EC-EARTH-SMHI-RCA4 and MPI-ESM-LR-CSIRO-CCAM (Fig. 12b). In particular, both RCMs show an increase in rainfall over all of EI for RCP 4.5 (Fig. 11b). The model ICHEC-EC-EARTH-SMHI-RCA4 shows an increased rainfall pattern with RCP 8.5 (Fig. 13a), while a huge decrease in seasonal rainfall is projected over the southern part of EI by other RCMs (Fig. 13b).

The model M7 reveals an increase in rainfall pattern over EI in both RCP4.5 and RCP8.5 scenarios for near and far futures, as shown in the above study. Other RCMs, on the other hand, have predicted a decline in seasonal rainfall patterns across the southern half of EI in the near and far future under RCP 4.5 and RCP 8.5 scenarios. The CORDEX-SA methodology evaluates regional climate models for their ability to simulate seasonal rainfall over EI. Validation was carried out on historical simulations from 1971 to 2005 and future forecasts from 2006 to 2070. Mishra et al. (2014) discovered that ICHEC-EC-EARTH-SMHI-RCA4 and LMDz-IITM-

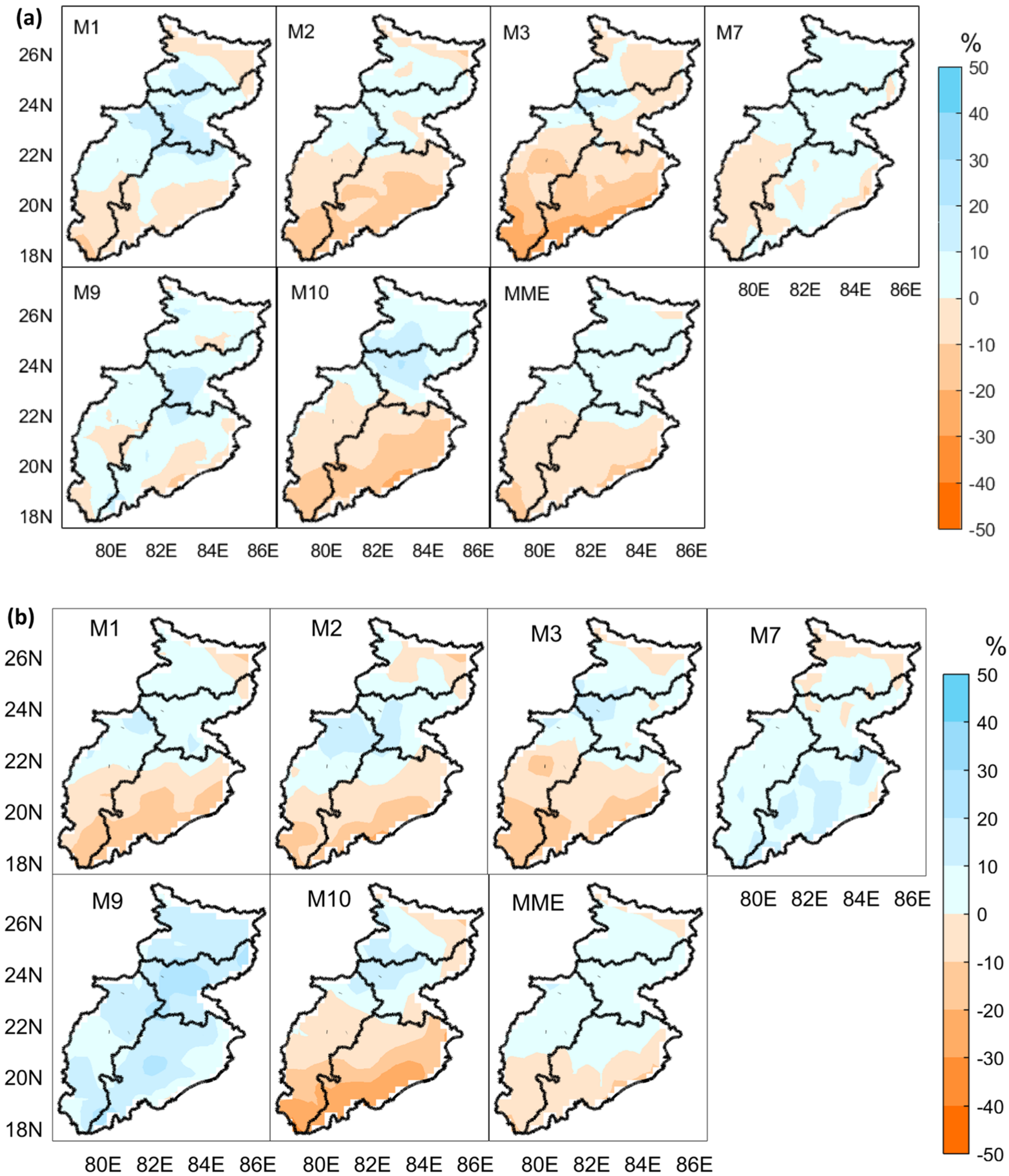

Figure 12
Percentage change in JJAS rainfall over EI based on present climate (1971–2005) for **a** near (2006–2040) and **b** far future (2041–2070) periods from the mean of six selected bias-corrected CORDEX-SA RCMs with RCP4.5 emission scenarios (**M1**: ACCESS-CSIRO-CCAM, **M2**: GFDL-CM3-CSIRO-CCAM, **M3**: CNRM-CM5-CSIRO-CCAM, **M4**: COSMO-CLM, **M5**: CCSM4CSIRO-CCAM, **M6**: GFDL-ESM2M-IITM-RegCM4, **M7**: ICHEC-EC-EARTH-SMHI-RCA4, **M8**: LMDz-IITM-RecCM4, **M9**: MPI-ESM-LR-CSIRO-CCAM and **M10**: NorESM1-M-CSIRO-CCAM)

RecCM4 have better simulations than their parent GCM and that the bias is enhanced after downscaling for COSMO-CLM and GFDL-ESM2M-IITM-RegCM4. COSMO-CLM, GFDL-ESM2M-IITM-RegCM4, LMDz-IITM-RecCM4, and ICHEC-EC-EARTH-SMHI-RCA4 were likewise shown to have a wet bias over EI. COSMO-CLM is the only RCM that is not hydrostatic. Notably, all of the CSIRO groups' RCMs have a dry bias for EI. According to Singh et al. (2017), the inability of RCM to depict Indian summer monsoon rainfall is not exclusively

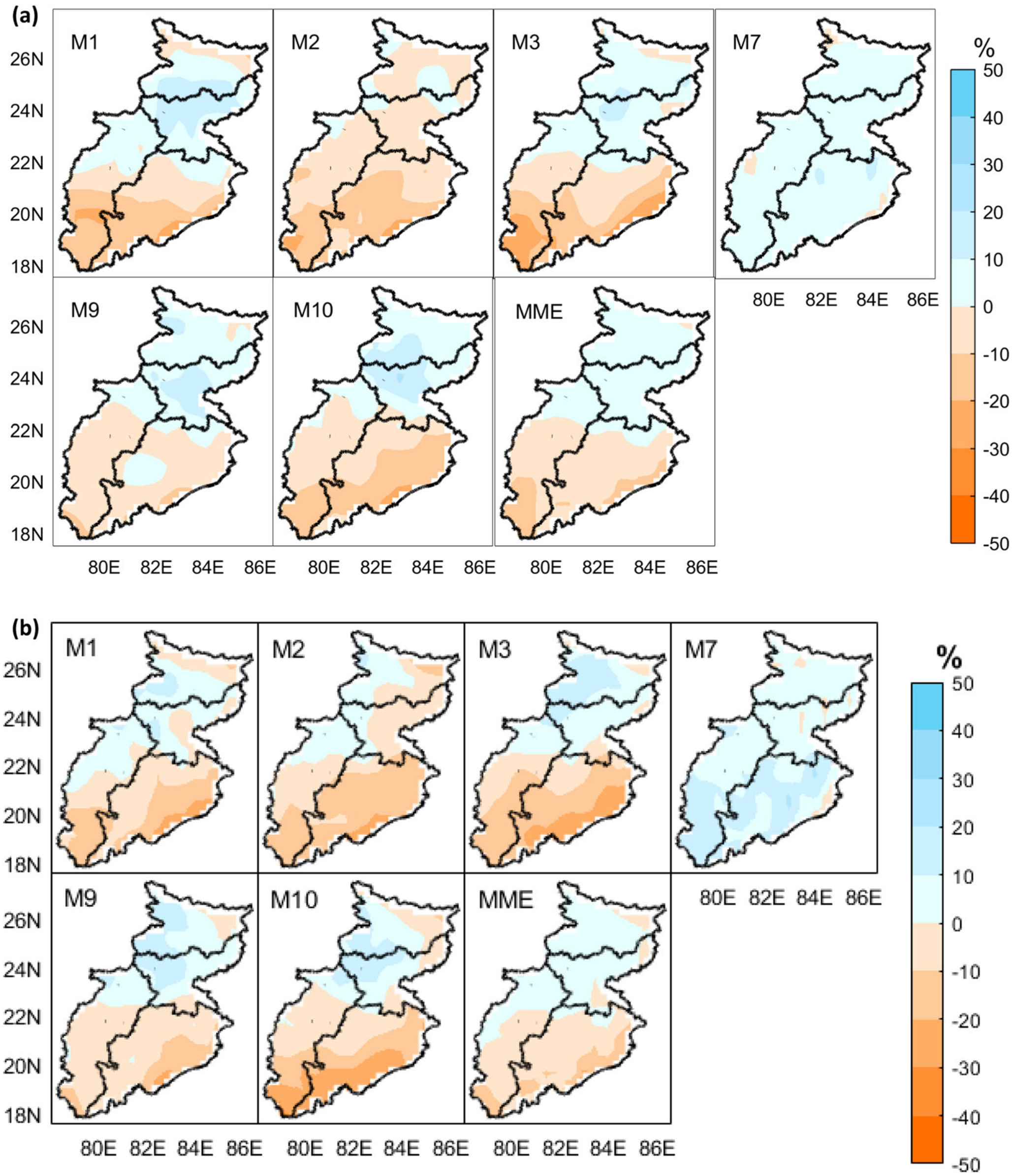

Figure 13
Percentage change in JJAS rainfall over EI based on present climate (1971–2005) for **a** near (2006–2040) and **b** far future (2041–2070) periods from mean of six selected bias-corrected CORDEX-SA RCMs with RCP8.5 emission scenarios (**M1**: ACCESS-CSIRO-CCAM, **M2**: GFDL-CM3-CSIRO-CCAM, **M3**: CNRM-CM5-CSIRO-CCAM, **M4**: COSMO-CLM, **M5**: CCSM4CSIRO-CCAM, **M6**: GFDL-ESM2M-IITM-RegCM4, **M7**: ICHEC-EC-EARTH-SMHI-RCA4, **M8**: LMDz-IITM-RecCM4, **M9**: MPI-ESM-LR-CSIRO-CCAM and **M10**: NorESM1-M-CSIRO-CCAM)

due to the parent GCM, but rather to poor modeling of land-sea interaction or a bad choice of nested area.

RCMs can now characterize weather patterns on a scale that is applicable to an entire region relatively better. However, RCMs are prone to systematic bias; thus, QQM methods have the potential to aid in reducing this bias. However, some limitations of QQM are addressed by Sunyer et al. (2015), including the fact that it is based on empirical distribution, the same correction is used for all seasons, and autocorrelation from the RCMs is not corrected but is instead impacted by the bias correction approach.

This restriction is not applicable because only one season is considered in this study.

4. Summary and Conclusions

The performance of ten RCMs from the CORDEX-SA experiment is examined in this study to simulate JJAS seasonal rainfall over EI from 1971 to 2005. The future projections for two time periods, near (2017–2040) and far (2041–2070), are obtained and described. Most of the CORDEX-SA regional climate model simulations accurately reproduce the JJAS seasonal rainfall pattern across EI; however, rainfall magnitudes are uncertain.

The CSIRO group's RCMs, i.e., ACCESS-CSIRO-CCAM, GFDL-CM3-CSIRO-CCAM, CNRM-CM5-CSIRO-CCAM, CCSM4-CSIRO-CCAM, MPI-ESM-LR-CSIRO-CCAM, and NorESM1-M-CSIRO-CCAM, can simulate the similar pattern but underestimate the magnitude of the seasonal rainfall for EI and other RCMs overestimating rainfall over some part of EI. The ICHEC-EC-EARTH-SMHI-RCA4 captures the spatial pattern of IAV and CV (%) of seasonal rainfall but is uncertain with magnitude. Also, the CSIRO group's RCMs show higher IAV over the southern part of EI instead of the central part of EI. IITM-RCMs, i.e., GFDL-ESM2M-IITM-RegCM4, and LMDz-IITM-RecCM4, have higher IAV over the eastern part of EI; COSMO-CLM shows high IAV over east and north EI, which is uncommon in other RCMs.

The standardized reconstruction and quantile mapping bias correction processes are quite good. They considerably improved the quality of CORDEX-SA RCM outputs in terms of portraying mean and interannual rainfall variability. For the present period (2006–2016), the bias-corrected data utilizing the Quantile mapping bias correction approach show strong agreement with IMD observations. Hence, the projections derived from this bias-corrected data indicate a good picture of the future climate over EI. According to the analysis of standardized anomalies of RCP 4.5 and RCP 8.5, JJAS seasonal rainfall will decrease in the near future (2017–2040) and rise in the far future (2041–2070) over EI.

The sub-grid process, mesoscale process, convective schemes used, land-atmosphere interaction in terms of heat and moisture exchange, and circulation pattern all contribute to the physics of a GCM, which in turn determines the performance of an RCM in terms of rainfall simulations. Even similar biases are present in both RCMs derived from the same parent GCMs (Kerkhoff et al., 2012; Wang, et al., 2004). Suppose the GCM's capacity to recreate a rainfall pattern across an area is restricted, and this weakness is passed on to the RCM. In that case, the RCM rainfall output will not reflect that region's proper rainfall distribution and pattern. As a result, improving the output of the GCM before dynamical downscaling is critical. Previous research has found that there is a considerable bias in rainfall outputs that varies from area to region (Kumar & Dimri, 2018; Choudhary & Dimri, 2018; Ghimire et al., 2018; Choudhary & Dimri, 2019; Sannan et al., 2020).

Because of the above analysis, it is possible to conclude that the change in JJAS rainfall over East India due to climate change exhibits a high degree of variability. In climate change studies, factors/conditions such as high population, dense forests, and rain-dependent regions are considered. The results presented in this study are only a qualitative indication of the range of expected JJAS rainfall changes over EI. By picking the appropriate models and subsequently changing them to depict rainfall for a local location better, this study may be valuable for the hydrological study across East India.

Acknowledgements

This research is the outcome of a research project entitled "Study of the Effects of Climate Change on Hydro-meteorological Processes: Droughts and Floods at Different Spatial and Temporal Scales in Eastern India" at IIT Bhubaneswar, sponsored by the Department of Science and Technology, Government of India. Authors duly acknowledge the India Meteorological Department (IMD) for providing a high-resolution gridded analysis dataset. The authors also thank the Climate Data Portal at the Center for Climate Change Research (CCCR), Indian Institute of Tropical Meteorology, India, for providing

CORDEX-SA data. The authors are also very appreciative of the anonymous reviewers for providing valuable suggestions and comments that helped improve the quality of the manuscript.

Data Availability

The IMD observation rainfall information is freely available on https://www.imdpune.gov.in/Clim_Pred_LRF_New/Grided_Data_Download.html for all India domain and CORDEX-SA regional climate models data are available on https://esgf-data.dkrz.de/search/cordex-dkrz/, The datasets extracted for East India and/or analyzed during the current study will be available from the corresponding author on request.

Code Availability

The code used for the study will be available from the corresponding author on request.

Declarations

Conflict of Interest The authors declare that they have no conflict of interest.

References

Acharya, N., Chattopadhyay, S., Mohanty, U. C., Dash, S. K., & Sahoo, L. N. (2013). On the bias correction of general circulation model output for Indian summer monsoon. *Meteorological Applications, 20*(3), 349–356. https://doi.org/10.1002/met.1294

Ajaaj, A. A., Mishra, A., & Khan, A. A. (2016). Comparison of BIAS correction techniques for GPCC rainfall data in semi-arid climate. *Stochastic Environmental Research and Risk Assessment, 30*(6), 1659–1675. https://doi.org/10.1007/s00477-015-1155-9

Barde, V., Nageswararao, M. M., Mohanty, U. C., Panda, R. K., & Ramadas, M. (2020). Characteristics of southwest summer monsoon rainfall events over East India. *Theoretical and Applied Climatology, 141*(3), 1511–1528. https://doi.org/10.1007/s00704-020-03251-y

Bhatla, R., Singh, M., Mall, R. K., Tripathi, A., & Raju, P. V. S. (2015). Variability of summer monsoon rainfall over Indo-Gangetic plains in relation to El-Nino/La-Nina. *Natural Hazards, 78*(2), 837–853. https://doi.org/10.1007/s11069-015-1746-2

Chaturvedi, R. K., Joshi, J., Jayaraman, M., Bala, G., & Ravindranath, N. H. (2012). Multi-model climate change projections for India under representative concentration pathways. *Current Science, 20*, 791–802.

Choudhary, A., & Dimri, A. P. (2019). On bias correction of summer monsoon precipitation over India from CORDEX-SA simulations. *International Journal of Climatology, 39*(3), 1388–1403. https://doi.org/10.1002/joc.5889

Choudhary, A., Dimri, A. P., & Maharana, P. (2018). Assessment of CORDEX-SA experiments in representing precipitation climatology of summer monsoon over India. *Theoretical and Applied Climatology, 134*(1), 283–307. https://doi.org/10.1007/s00704-017-2274-7

Das, P. K., Dutta, D., Sharma, J. R., & Dadhwal, V. K. (2016). Trends and behaviour of meteorological drought (1901–2008) over Indian region using standardized precipitation–evapotranspiration index. *International Journal of Climatology, 36*(2), 909–916. https://doi.org/10.1002/joc.4392

Dey, P., & Sarkar, A. K. (2011). Revisiting indigenous farming knowledge of Jharkhand (India) for conservation of natural resources and combating climate change.

Dimri, A. P., Kumar, D., Chopra, S., & Choudhary, A. (2019). Indus River Basin: Future climate and water budget. *International Journal of Climatology, 39*(1), 395–406. https://doi.org/10.1002/joc.5816

Dimri, A. P., Kumar, D., Choudhary, A., & Maharana, P. (2018a). Future changes over the Himalayas: Mean temperature. *Global and Planetary Change, 162*, 235–251. https://doi.org/10.1016/j.gloplacha.2018.01.014

Dimri, A. P., Kumar, D., Choudhary, A., & Maharana, P. (2018b). Future changes over the Himalayas: Maximum and minimum temperature. *Global and Planetary Change, 162*, 212–234. https://doi.org/10.1016/j.gloplacha.2018.01.015

Dobler, A., & Ahrens, B. (2010). Analysis of the Indian summer monsoon system in the regional climate model COSMO-CLM. *Journal of Geophysical Research Atmospheres, 115*, D16. https://doi.org/10.1029/2009JD013497

Ebert, E. E., & McBride, J. L. (2000). Verification of precipitation in weather systems: Determination of systematic errors. *Journal of Hydrology, 239*(1–4), 179–202. https://doi.org/10.1016/S0022-1694(00)00343-7

Enayati, M., Bozorg-Haddad, O., Bazrafshan, J., Hejabi, S., & Chu, X. (2021). Bias correction capabilities of quantile mapping methods for rainfall and temperature variables. *Journal of Water and Climate Change, 12*(2), 401–419. https://doi.org/10.2166/wcc.2020.261

Fowler, H. J., Blenkinsop, S., & Tebaldi, C. (2007). Linking climate change modelling to impacts studies: Recent advances in downscaling techniques for hydrological modelling. *International Journal of Climatology A Journal of the Royal*

Meteorological Society, 27(12), 1547–1578. https://doi.org/10.1002/joc.1556

Ghimire, S., Choudhary, A., & Dimri, A. P. (2018). Assessment of the performance of CORDEX-South Asia experiments for monsoonal precipitation over the Himalayan region during present climate: Part I. *Climate Dynamics, 50*(7), 2311–2334. https://doi.org/10.1007/s00382-015-2747-2

Giorgi, F., Jones, C., & Asrar, G. R. (2009). Addressing climate information needs at the regional level: The CORDEX framework. *World Meteorological Organization Bulletin, 58*(3), 175.

Kerkhoff, C., Künsch, H. R., & Schär, C. (2012). Relations between RCMs and GCMs in the ENSEMBLES simulations. In EGU General Assembly Conference Abstracts (p. 1873).

Kulkarni, A. (2012). Weakening of Indian summer monsoon rainfall in warming environment. *Theoretical and Applied Climatology*, *109*, 447–459. https://doi.org/10.1007/s00704-012-0591-4

Kumar, A., Dudhia, J., Rotunno, R., Niyogi, D., & Mohanty, U. C. (2008). Analysis of the 26 July 2005 heavy rain event over Mumbai, India using the Weather Research and Forecasting (WRF) model. *Quarterly Journal of the Royal Meteorological Society, 134*(636), 1897–1910. https://doi.org/10.1002/qj.325

Kumar, D., & Dimri, A. P. (2018). Regional climate projections for Northeast India: An appraisal from CORDEX South Asia experiment. *Theoretical and Applied Climatology, 134*(3), 1065–1081. https://doi.org/10.1007/s00704-017-2318-z

Kumar, K. K., Patwardhan, S. K., Kulkarni, A., Kamala, K., Rao, K. K., & Jones, R. (2011). Simulated projections for summer monsoon climate over India by a high-resolution regional climate model (PRECIS). *Current Science, 20*, 312–326.

Kumar, K. N., Rajeevan, M., Pai, D. S., Srivastava, A. K., & Preethi, B. (2013). On the observed variability of monsoon droughts over India. *Weather and Climate Extremes, 1*, 42–50. https://doi.org/10.1016/j.wace.2013.07.006

Mallya, G., Mishra, V., Niyogi, D., Tripathi, S., & Govindaraju, R. S. (2016). Trends and variability of droughts over the Indian monsoon region. *Weather and Climate Extremes, 12*, 43–68. https://doi.org/10.1016/j.wace.2016.01.002

Meshram, S. G., Singh, V. P., & Meshram, C. (2017). Long-term trend and variability of precipitation in Chhattisgarh State. *India. Theoretical and Applied Climatology, 129*(3), 729–744. https://doi.org/10.1007/s00704-016-1804-z

Mishra, V., Kumar, D., Ganguly, A. R., Sanjay, J., Mujumdar, M., Krishnan, R., & Shah, R. D. (2014). Reliability of regional and global climate models to simulate precipitation extremes over India. *Journal of Geophysical Research Atmospheres, 119*(15), 9301–9323. https://doi.org/10.1002/2014JD021636

Mishra, V., Smoliak, B. V., Lettenmaier, D. P., & Wallace, J. M. (2012). A prominent pattern of year-to-year variability in Indian Summer Monsoon Rainfall. *Proceedings of the National Academy of Sciences, 109*(19), 7213–7217. https://doi.org/10.1073/pnas.1119150109

Mohanty, U. C., Nageswararao, M. M., Sinha, P., Nair, A., Singh, A., Rai, R. K., & Dash, G. P. (2019). Evaluation of performance of seasonal precipitation prediction at regional scale over India. *Theoretical and Applied Climatology, 135*(3), 1123–1142. https://doi.org/10.1007/s00704-018-2421-9

Moss, R. H., Edmonds, J. A., Hibbard, K. A., Manning, M. R., Rose, S. K., Van Vuuren, D. P., & Wilbanks, T. J. (2010). The next generation of scenarios for climate change research and assessment. *Nature, 463*(7282), 747–756. https://doi.org/10.1038/nature08823

Nageswararao, M. M., Mohanty, U. C., Osuri, K. K., & Ramakrishna, S. S. V. S. (2016b). Prediction of winter precipitation over northwest India using ocean heat fluxes. *Climate Dynamics, 47*(7), 2253–2271. https://doi.org/10.1007/s00382-015-2962-x

Nageswararao, M. M., Mohanty, U. C., Ramakrishna, S. S. V. S., & Dimri, A. P. (2018). An intercomparison of observational precipitation data sets over Northwest India during winter. *Theoretical and Applied Climatology, 132*(1), 181–207. https://doi.org/10.1007/s00704-017-2083-z

Nageswararao, M. M., Mohanty, U. C., Ramakrishna, S. S. V. S., Nair, A., & Prasad, S. K. (2016a). Characteristics of winter precipitation over Northwest India using high-resolution gridded dataset (1901–2013). *Global and Planetary Change, 147*, 67–85. https://doi.org/10.1016/j.gloplacha.2016.10.017

Nageswararao, M. M., Sannan, M. C., & Mohanty, U. C. (2019a). Characteristics of various rainfall events over South Peninsular India during northeast monsoon using high-resolution gridded dataset (1901–2016). *Theoretical and Applied Climatology, 137*(3), 2573–2593. https://doi.org/10.1007/s00704-018-02755-y

Nageswararao, M. M., Sinha, P., Mohanty, U. C., Panda, R. K., & Dash, G. P. (2019b). Evaluation of district-level rainfall characteristics over Odisha using high-resolution gridded dataset (1901–2013). *SN Applied Sciences, 1*(10), 1–24. https://doi.org/10.1007/s42452-019-1234-5

Nath, R., Nath, D., Li, Q., Chen, W., & Cui, X. (2017). Impact of drought on agriculture in the Indo-Gangetic Plain. *India. Advances in Atmospheric Sciences, 34*(3), 335–346. https://doi.org/10.1007/s00376-016-6102-2

Pai, D. S., Rajeevan, M., Sreejith, O. P., Mukhopadhyay, B., & Satbha, N. S. (2014). Development of a new high spatial resolution (0.25× 0.25) long period (1901–2010) daily gridded rainfall data set over India and its comparison with existing data sets over the region. *Mausam, 65*(1), 1–18. https://doi.org/10.54302/mausam.v65i1.851

Pai, D. S., Sridhar, L., Badwaik, M. R., & Rajeevan, M. (2015). Analysis of the daily rainfall events over India using a new long period (1901–2010) high resolution (0.25 × 0.25) gridded rainfall data set. *Climate Dynamics, 45*(3), 755–776. https://doi.org/10.1007/s00382-014-2307-1

Parth Sarthi, P., Kumar, P., & Ghosh, S. (2016). Possible future rainfall over Gangetic Plains (GP), India, in multi-model simulations of CMIP3 and CMIP5. *Theoretical and Applied Climatology, 124*(3), 691–701. https://doi.org/10.1007/s00704-015-1447-5

Patwardhan, S., Kulkarni, A., & Sabade, S. (2016). Projected changes in semi permanent systems of Indian summer monsoon in CORDEX-SA framework. *American Journal of Climate Change, 5*(2), 133–146. https://doi.org/10.4236/ajcc.2016.52013

Quamar, M. F., & Bera, S. K. (2017). Pollen records related to vegetation and climate change from northern Chhattisgarh, central India during the late Quaternary. *Palynology*. https://doi.org/10.1080/01916122.2015.1077172

Rajeevan, M., & Nanjundiah, R. S. (2009). Coupled model simulations of twentieth century climate of the Indian summer monsoon. *Platinum Jubilee Special Volume of the Indian Academy of Sciences, 20*, 537–568.

Rockel, B. (2015). The regional downscaling approach: A brief history and recent advances. *Current Climate Change Reports, 1*(1), 22–29. https://doi.org/10.1007/s40641-014-0001-3

Roxy, M. K., Ghosh, S., Pathak, A., Athulya, R., Mujumdar, M., Murtugudde, R., & Rajeevan, M. (2017). A threefold rise in widespread extreme rain events over central India. *Nature Communications, 8*(1), 1–11. https://doi.org/10.1038/s41467-017-00744-9

Sahany, S., Venugopal, V., & Nanjundiah, R. S. (2010). The 26 July 2005 heavy rainfall event over Mumbai: Numerical modeling aspects. *Meteorology and Atmospheric Physics, 109*(3), 115–128. https://doi.org/10.1007/s00703-010-0099-3

Sannan, M. C., Nageswararao, M. M., & Mohanty, U. C. (2020). Performance evaluation of CORDEX-South Asia simulations and future projections of northeast monsoon rainfall over south peninsular India. *Meteorology and Atmospheric Physics, 132*(5), 743–770. https://doi.org/10.1007/s00703-019-00716-2

Seenirajan, M., Natarajan, M., Thangaraj, R., & Bagyaraj, M. (2017). Study and analysis of Chennai flood 2015 using GIS and multicriteria technique. *Journal of Geographic Information System, 9*(02), 126. https://doi.org/10.4236/jgis.2017.92009

Sharma, S., & Singh, P. K. (2017). Long term spatiotemporal variability in rainfall trends over the state of Jharkhand, India. *Climate, 5*(1), 18. https://doi.org/10.3390/cli5010018

Sharmila, S., Joseph, S., Sahai, A. K., Abhilash, S., & Chattopadhyay, R. (2015). Future projection of Indian summer monsoon variability under climate change scenario: An assessment from CMIP5 climate models. *Global and Planetary Change, 124*, 62–78. https://doi.org/10.1016/j.gloplacha.2014.11.004

Singh, A., Sahoo, R. K., Nair, A., Mohanty, U. C., & Rai, R. K. (2017). Assessing the performance of bias correction approaches for correcting monthly precipitation over India through coupled models. *Meteorological Applications, 24*(3), 326–337. https://doi.org/10.1002/met.1627

Slater, A. G., & Lawrence, D. M. (2013). Diagnosing present and future permafrost from climate models. *Journal of Climate, 26*(15), 5608–5623. https://doi.org/10.1175/JCLI-D-12-00341.1

Sunyer, M. A., Hundecha, Y., Lawrence, D., Madsen, H., Willems, P., Martinkova, M., & Yücel, I. (2015). Inter-comparison of statistical downscaling methods for projection of extreme precipitation in Europe. *Hydrology and Earth System Sciences, 19*(4), 1827–1847. https://doi.org/10.5194/hess-19-1827-2015

Swain, M., Pattanayak, S., & Mohanty, U. C. (2018). Characteristics of occurrence of heavy rainfall events over Odisha during summer monsoon season. *Dynamics of Atmospheres and Oceans, 82*, 107–118. https://doi.org/10.1016/j.dynatmoce.2018.05.004

Tang, J., Niu, X., Wang, S., Gao, H., Wang, X., & Wu, J. (2016). Statistical downscaling and dynamical downscaling of regional climate in China: Present climate evaluations and future climate projections. *Journal of Geophysical Research Atmospheres, 121*(5), 2110–2129. https://doi.org/10.1002/2015JD023977

Taylor, K. E., Stouffer, R. J., & Meehl, G. A. (2012). An overview of CMIP5 and the experiment design. *Bulletin of the American Meteorological Society, 93*(4), 485–498. https://doi.org/10.1175/BAMS-D-11-00094.1

Tesfaye, K., Aggarwal, P. K., Mequanint, F., Shirsath, P. B., Stirling, C. M., Khatri-Chhetri, A., & Rahut, D. B. (2017). Climate variability and change in Bihar, India: Challenges and opportunities for sustainable crop production. *Sustainability, 9*(11), 1998. https://doi.org/10.3390/su9111998

Wang, Y., Leung, L. R., McgregoR, J. L., Lee, D. K., Wang, W. C., Ding, Y., & Kimura, F. (2004). Regional climate modeling: Progress, challenges, and prospects. *Journal of the Meteorological Society of Japan, Ser. II, 82*(6), 1599–1628. https://doi.org/10.2151/jmsj.82.1599

Warwade, P., Tiwari, S., Ranjan, S., Chandniha, S. K., & Adamowski, J. (2018). Spatio-temporal variation of rainfall over Bihar State, India. *Journal of Water and Land Development*. https://doi.org/10.2478/jwld-2018-0018

Wehner, M. F., Smith, R. L., Bala, G., & Duffy, P. (2010). The effect of horizontal resolution on simulation of very extreme US precipitation events in a global atmosphere model. *Climate Dynamics, 34*(2), 241–247. https://doi.org/10.1007/s00382-009-0656-y

Wilby, R. L., & Wigley, T. M. (1997). Downscaling general circulation model output: A review of methods and limitations. *Progress in Physical Geography*, *21*(4), 530–548.

(Received May 24, 2022, revised December 8, 2022, accepted December 22, 2022, Published online January 21, 2023)